BILINGUAL PUBLISHING CO.
Pioneer of Global Academics Since 1984

Non-Metallic Material Science
https://ojs.bilpublishing.com/index.php/nmms

ARTICLE

The Effect of ZnO on the Physicochemical and Mechanical Properties of Aluminosilicate Dental Cements

Z. Kahrobaee M. Mazinani F. Kermani S. Mollazadeh*

Department of Materials Engineering, Faculty of Engineering, Ferdowsi University of Mashhad (FUM), Azadi Sq, Mashhad, Iran

ARTICLE INFO

Article history
Received: 6 October 2021
Accepted: 22 October 2021
Published Online: 31 October 2021

Keywords:
Aluminosilicate glasses
Glass ionomer cement (GIC)
ZnO
Orthodontic applications

ABSTRACT

In this study, the effect of the addition of various amounts of ZnO (0, 1, 2, and 3 wt. %) to aluminosilicate bioactive glass (BGs) network (SiO_2-Al_2O_3-P_2O_5-CaF_2-CaO-K_2O-Na_2O) on the mechanical properties of the fabricated glass ionomer cement (GIC) samples was studied. The GIC samples were fabricated by mixing the synthesized aluminosilicate BGs with Riva-self cure liquid. The synthesized aluminosilicate glass was characterized using differential thermal analysis (DTA), X-Ray diffraction (XRD), Fourier-transform infrared spectroscopy (FTIR), and scanning electron microscopy (SEM). Besides, the mechanical properties of GICs were evaluated using Vickers microhardness and Diametral tensile strength (DTS) test. According to DTA analysis, the glass transition temperature (Tg) of aluminosilicate BGs was decreased from 575 to 525 °C. According to the results, the aluminosilicate BGs with an amorphous state (~90%) and the grain size of 36 μm were synthesized. Doping of the ZnO to glass network up to 3 wt. % could increase the amorphous phase up to 95% and decrease the grain size of the particles up to 28 μm. The microhardness and DTS of the GIC samples containing the aluminosilicate BGs were about 677 Hv and 8.5 MPa, respectively. Doping of ZnO to the glass network increased the mentioned values up to 816 Hv and 12.1 MPa, respectively.

1. Introduction

Glass Ionomer Cements (GICs) are a group of biocompatible atraumatic restorative materials which have been widely used to repair damaged teeth [1]. GICs consist mainly of bioactive glass (BGs) (e.g., calcium alumino-fluoro-silicate glass) powder and an aqueous solution containing polyacrylic acid [2]. The GICs have the remarkable ability to develop an ion-exchange hydroxyapatite layer and uptake of fluoride ions which can enhance their adherence to the tooth and the metal substrate [3]. GICs can also release fluoride ions due to their specific chemical composition [4]. Furthermore, their low cytotoxicity and low coefficient of thermal expansion,

**Corresponding Author:*
S. Mollazadeh,
Department of Materials Engineering, Faculty of Engineering, Ferdowsi University of Mashhad (FUM), Azadi Sq, Mashhad, Iran;
Email: Mollazadeh.b@um.ac.ir

DOI: https://doi.org/10.30564/nmms.v3i2.3806
Copyright © 2021 by the author(s). Published by Bilingual Publishing Co. This is an open access article under the Creative Commons Attribution-NonCommercial 4.0 International (CC BY-NC 4.0) License. (https://creativecommons.org/licenses/by-nc/4.0/).

which is close to that of the enamel, have made them be desirable dental restorative materials [5,6]. However, due to the relatively short lifetime and poor mechanical properties of these materials, their application has encountered some limitations [5,6]. Mechanical properties of GICs have been affected by altering the composition of the polymeric matrix or the filler material [7]. Since GICs are brittle, any inhomogeneity produced during manufacturing can potentially be a defect resulting in a catastrophic failure [7]. Therefore, controlling and improving the composition of aluminosilicate BGs is necessary to overcome the challenge of GICs [8].

A new formulation of GICs -with relevant properties and applications- with the incorporation of some agents to GICs based-formulation was used to improve/generate self-adhesive, esthetically pleasing, and antibacterial properties [9-11]. These improvements could be involved in decreasing the incidence of recurrent caries [9]. Several investigations have been conducted in order to produce GICs with better mechanical properties through the modification of polymeric matrix [12]. Besides, the application of various filler materials was investigated to improve the mechanical properties of GICs [13]. Among these investigations, few studies have been focused on the composition of base aluminosilicate BGs particles. The presence of a second phase, mostly a ceramic, can improve mechanical properties; however, crystallization of ceramic crystalline phase causes some challenges for the glass system in which the setting reaction of GIC may be hindered [13]. Therefore, the effect of altering the compositions on the physicochemical and structural properties of glass has been considered in this investigation. It is believed that silicon and phosphorus existing in the amorphous matrix of the glass can form an inorganic framework which makes the cement durable in aqueous environments and improves its final mechanical properties [14]. The effect of additives on the mechanical properties of dental cement should be clarified through the well-designed study.

Zinc oxide (ZnO) is a well-known oxide in culturing bone tissue [15]. Also, zinc ions are vital for correcting the function of the immune system [16]. Zinc can be beneficial for dental decay due to its antibacterial properties [17-19]. The Zn-O-P structural groups could substitute with Ca-O-P gropes of aluminosilicate glass network [20]. Consequently, the mechanical properties of the BGs could be altered. The effect of ZnO on the properties of aluminosilicate BGs and the mechanical properties of GICs should be clarified.

In the current study, the effect of adding different amounts of ZnO (1,2, and 3 wt.%) to the properties of melt-quench aluminosilicate BGs containing Al_2O_3, SiO_2, CaF_2, P_2O_5, CaO, K_2O, Na_2O components was studied. The effect of ZnO doping on the properties of melt-quench glass was studied using differential thermal (DTA), X-ray diffraction (XRD), Fourier transform infrared (FTIR), and scanning electron microscopy (SEM). Besides, the GICs samples were fabricated by mixing the synthesized aluminosilicate BGs with Riva-self cure liquid to clarify the role of ZnO on the mechanical properties of dental cement. The effect of ZnO addition on the mechanical properties of GIC was investigated using Vickers microhardness and Diametral Tensile Stress (DTS).

2. Materials and Method

2.1 Glass Synthesis

The compositions of BGs systems are presented in Table 1. The glass samples were prepared using the reagent grade powders containing alumina (Al_2O_3, 99.9%, Merck, Germany), quartz (SiO_2, 99.9%, Merck, Germany), calcium Fluoride (CaF_2, 99%, Merck, Germany), mono-ammonium phosphate (MAP, 98%, Merck, Germany), calcium carbonate ($CaCO_3$, 8.9%, Merck, Germany), zinc oxide (ZnO, 99%, Merck, Germany), potassium carbonate (K_2CO_3, 99%) and sodium carbonate (Na_2CO_3, 99%).

The components of the samples were accurately weighed and mixed thoroughly in a porcelain mixer for about 30 min. The weighed samples were melted in an electrically heated furnace in alumina crucibles with a heating rate of 10 °C/min to 1450 °C and heated for 2h. Frits were obtained by quenching the melt samples in water at 25 °C. After quenching, frits were dried and then milled in a high-speed porcelain ball mill for 30 min. The glass samples were labeled according to their approximate

Table 1. Composition of the synthesized BGs in wt. %.

Sample	Al_2O_3	SiO_2	CaF_2	P_2O_5	CaO	ZnO	K_2O	Na_2O
0%	33	24	21.6	18.7	9.8	0	3	1.98
1%	33	24	21.6	18.7	9.8	1	3	1.98
2%	33	24	21.6	18.7	9.8	2	3	1.98
3%	33	24	21.6	18.7	9.8	3	3	1.98

ZnO content, i.e., 0, 1, 2, and 3 wt.% ZnO for the samples.

2.2 GIC Samples Preparation

In order to prepare GIC samples, each synthesized glass and Riva self-cure liquid polymer (powder to polymer volume ratio 3.8) were mixed in a porcelain mixer for 15 min. The cylindrical specimens were prepared according to ASTM D3967 with 6 mm diameter and thickness of 4 mm. The schematic presentation of the BGs synthesis and the fabrication of GIC samples is shown in Figure 1.

2.3 Characterizations

The effect of ZnO on the thermal behavior of BGs samples was analyzed using differential thermal (DTA) analyses (STA 503, BAHR, Germany) with a heating rate of 10 °C/min in air. X-ray diffraction (XRD) (X'Pert PW 3040/60 Philips, Netherland) at the range of 2θ=20-70° was used to identify the phase compositions of powder. Fourier transform infrared (FTIR) analysis at the range of 400-4000 cm^{-1} (Avatar 370, USA) were conducted to examine the chemical bonds of the synthesized BGs. The morphology of synthesized BGs and the GIC samples were determined using scanning electron microscopy (SEM) (Vp-1450-Leo, Germany).

The microhardness of GIC samples was evaluated by using the Vickers microhardness (MITECH HV-1000, co LTD, China) test. To do this test, the load of 50 gr-f and the holding time of 20 seconds were used. The diametrical tensile stress (DTS) was performed according to ASTM D3967 by using SANTAM STM-20 tensile machine with a crosshead speed of 0.5 mm/min.

2.4 Statistical Analysis

The micro-hardness and DTS tests were performed at latest 8 times and the data were represented as mean ± standard deviation. The data was statistically analyzed via the one-way ANOVA analysis (GraphPad Prism, 9.1.0 (221), USA) followed by post hoc analysis (*p ≤ 0.05, **p ≤ 0.01, ***p ≤ 0.001, ****p ≤ 0.0001). The correlation matrix presentation of the data was calculated using Origin software (version 2021b). The type of correlation plot was Pearson and the significant level (* p < 0.05) was specified.

3. Results and Discussion

3.1 DTA Analysis

The DTA analysis results of the BGs samples are shown in Figure 1. The summary of characterized temperatures containing glass transition temperate (T_g) and the first and second crystallization temperature (T_{c1} and T_{c2}) are summarized in Table 2. According to obtained data, it can be said that the T_g and the crystallization temperatures of the BGs were decreased by increasing the amount of ZnO up to 3 wt.%. The T_g of un-doped BGs, doped BGs with 1, 2, and 3 wt.% of ZnO were about 575, 575, 550, and 525 °C, respectively. Decreasing the T_g of the doped samples is related to changing the glass network [21]. Ca^{2+} ions (ionic raids 231 pm) could substitute with Zn^{2+} ions (ionic radius 74 pm) in the glass network. Doping of the structure could decrease its stability due to increasing the lattice strain and increasing the entropy of BGs, as reported in [22,23]. Consequently, in line with which was observed in this

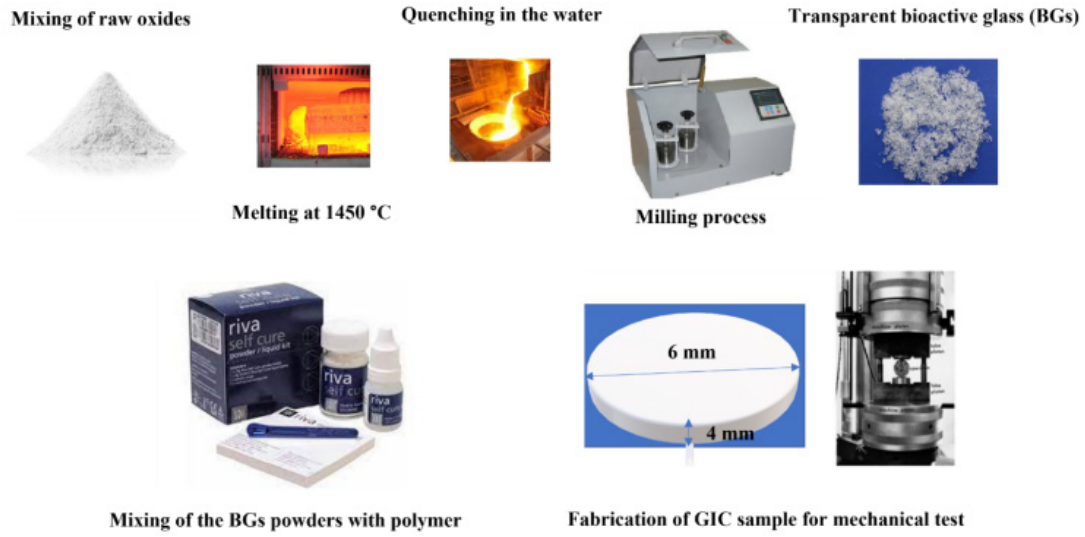

Figure 1. Schematic representation of the BGs synthesis and the fabrication of GIC

study, the substitution of ZnO instead of CaO decreased the T_g and the crystallization temperatures.

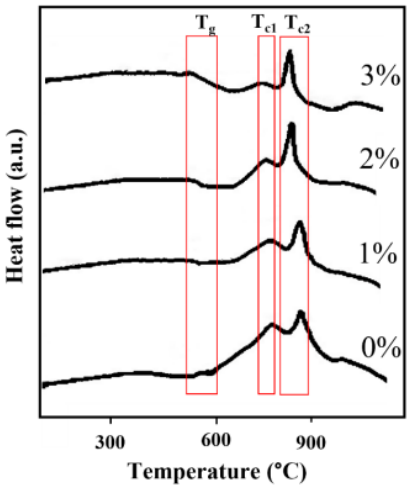

Figure 1. The results of DTA analysis of the synthesized BGs.

Table 2. The glass transition temperature (T_g) and first and second crystallization temperature (T_{c1} and T_{c2}).

Sample	T_g °C	T_{c1} °C	T_{c2} °C
0%	575	785	870
1%	575	775	840
2%	550	775	850
3%	525	750	825

3.2 XRD and FTIR Analyses

The XRD results of BGs after quenching are represented in Figure 2. According to the diffraction patterns, all samples have shown an amorphous state. The results of the calculation of the crystallinity of the samples are presented in Table 3. According to the data, the crystallinity of the samples was decreased by increasing the amount of ZnO. The crystallinity degree of un-doped BGs, doped BGs with 1, 2, and 3 wt.% of ZnO were about 11, 8, <5, and <5 %, respectively. As reported, doping of agents to multi-components BGs, could increase the network' complexity of the glass [21]. Increasing the complexity of glass structure due to increasing the density of bridging oxygen at the effect of doping of agents (in this study, ZnO) could prevent the crystallization of glass [24,25].

The major FTIR bands of the samples are shown in Figure 3. The marked bands over the range of 450-480 cm^{-1} are related to bending vibration of O-Si-O groups in the non-bridging oxygen (NBO) sites of SiO_4^{4-} tetrahedral structure [26]. The broad bands around 1000 cm^{-1} are related to Si-O-Si groups [26]. The marked bands over the range of 640-750 cm^{-1} are related to the Al-O structural groups of aluminosilicate BGs [10,27].

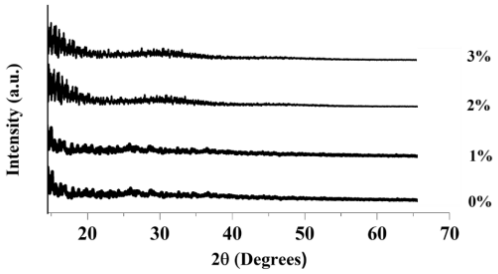

Figure 2. The results of XRD analysis of the synthesized BGs.

Table 3: The crystallinity and grain size of the synthesized BGs.

Sample	Crystallinity (%)	Grain size (μm)
0%	11	36 ± 5
1%	8	35 ± 4
2%	< 5	32 ± 2
3%	< 5	28 ± 2

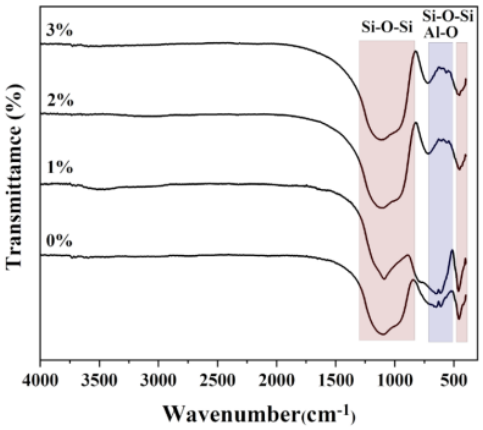

Figure 3. The results of FTIR analysis of the synthesized BGs.

3.3. SEM Micrographs

The SEM micrographs of the synthesized BGs are represented in Figure 4. According to these figures, all glass has an irregular shape and morphology, stating the amorphous state of the samples, as XRD patterns (see Figure 3) illustrated. The irregular shape morphology of the melt-quench synthesized BGs was also observed in [28]. The average grain size values of the synthesized BGs are repressed in Table 3. According to the data, adding ZnO to BGs could decrease the grain size of the BGs. The grain size of un-doped BGs, doped BGs with 1, 2, and 3 wt.% of ZnO were about 36, 35, 32, and 28 μm,

respectively. According to the literature [29,30], doping of ZnO to BGs prevents grain growth as well as increasing the homogeneity of grain distributions. Besides, the lower ionic radius of Zn^{2+} than Ca^{2+} in which Ca^{2+} substituted with Ca^{2+} in the glass network could decrease the final grain size of the particles.

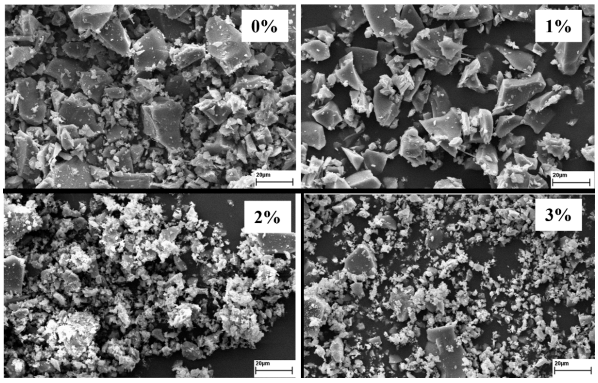

Figure 4. The results of SEM analysis of the synthesized BGs.

3.4 Microhardness

The results of the microhardness of GIC samples are represented in Figure 5 and Table 4. The significant changes were marked based on P values (*p ≤ 0.05, **p ≤ 0.01, ***p ≤ 0.001, ****p ≤ 0.0001) in Figure 5. According to the data, the microhardness values of the GIC sample containing un-doped BGs, doped BGs with 1, 2, and 3 wt.% of ZnO were about 677, 770, 816, and 775 Hv, respectively. Increasing the microhardness to an optimum value could be related to smaller grain size and better particle size distribution of the BGs particles [31]. As reported in [32], the dopants are distributed at the bulk and the surface of the BGs. It is assumed that some amounts of the dopants play as the functionalization agents at the BGs surface (see ref [33]) and could diffuse and accumulate on the Stern layer of the glass structure, as shown in the schematic representation of Figure 6. Besides, increasing the concentration of the dopants could generate the surface defects such as oxygen vacancies on the glass surface; these defects could enhance the mechanical and biological properties of the glass [34]. These phenomena could contribute to obtaining a homogenous structure of GIC samples. Besides, the lower ionic radius of Zn^{2+} ion than Ca^{2+} resulted in the formation of stronger bonds with oxygen atoms in the structure of BGs. Decreasing the crystallinity degree of BGs at the effect of ZnO could also increase the microhardness values of GIC samples in line with the previous study [31,35,36]. In summary, the homogenous distribution of BGs in the polymeric substrate and the smaller particles size of the samples could increase the microhardness of the samples. It's noted that the different particles size and various distribution of particles at the effect of additives directly affected the morphology of GIC samples (Figure 8) and could be altered microhardness.

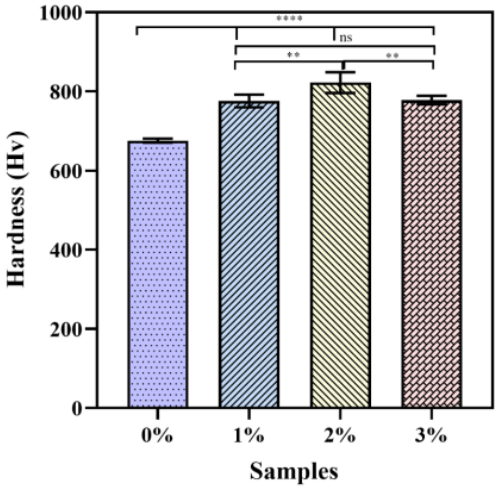

Figure 5. The results of statistical analysis of microhardness of GIC samples.

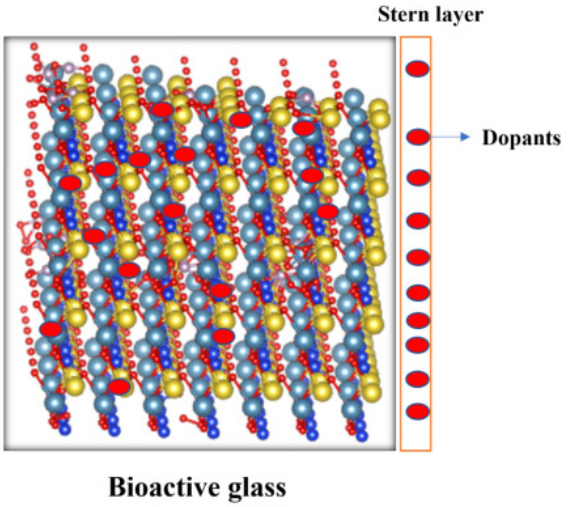

Figure 6. The schematic representation of the accumulation of Zn^{2+} ions on the Stern layer of BGs.

Table 4. The microhardness results of GIC samples.

Samples	Number of Samples	Average microhardness (Hv)
0%	8	677 ± 15
1%	8	770 ± 12
2%	8	816 ± 10
3%	8	775 ± 11

3.5 Diametral Tensile Stress (DTS)

The average values of fracture stress of GIC samples are represented in Table 5 and Figure 7. The significant changes were marked based on P values (*p ≤ 0.05, **p ≤ 0.01, ***p ≤ 0.001, ****p ≤ 0.0001) in Figure 7. According to the data, the microhardness values of the GIC sample containing un-doped, doped with 1, 2, and 3 wt.% of ZnO were about 8.5, 11.8, 12.1, and 11.7 MPa, respectively. According to the previous sections that indicated increasing the amounts of amorphous phase with increasing the amount of ZnO, the higher mechanical properties of GIC containing ZnO-doped BGs was expected as reported in [37,38]. Besides, ZnO could improve the formed inorganic framework of silicon and phosphorous in the glass structure and mechanical properties [17]. SEM micrographs of the fracture surface are shown in Figure 8. According to these figures, the main defect in the samples was the cavities. These cavities are probably air bubbles that have been formed during composite preparation techniques [39].

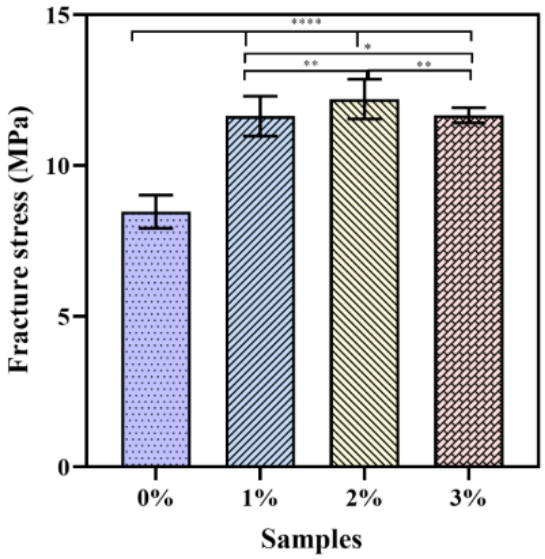

Figure 7. The results of statistical analysis of fracture stress of GIC samples.

Table 5. The average fracture stresses of GIC samples

Sample	Number of samples	Average fracture stress (MPa)
0%	8	8.5 ± 1.5
1%	8	11.8 ± 1.2
2%	8	12.1 ± 1.6
3%	8	11.7 ± 1.3

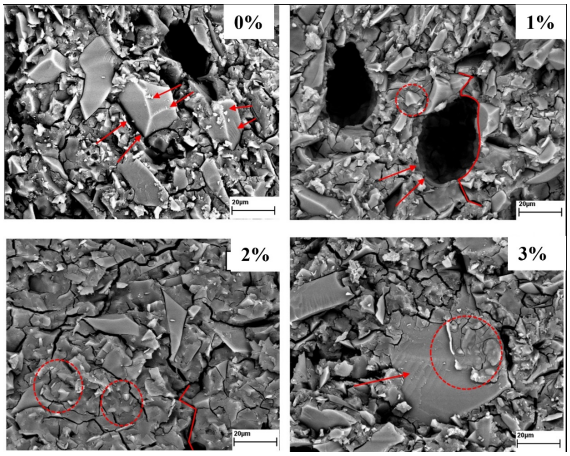

Figure 8. The SEM micrographs of the fracture surface of BGs.

3.6 Correlation Matrix Presentation of the Data

Correlation matrix presentation is a simple way to show the relationship between the obtained porpoise of materials [40]. The correlation matrix of the data was calculated and presented in Figure 9. According to this matrix, it can be said that increasing the amount of ZnO to the BGs network could directly increase the hardness and fracture stress of the GIC samples. Besides, the direct and significant relation of grain size values of the synthesized glass with the mechanical properties of the GIC was observed.

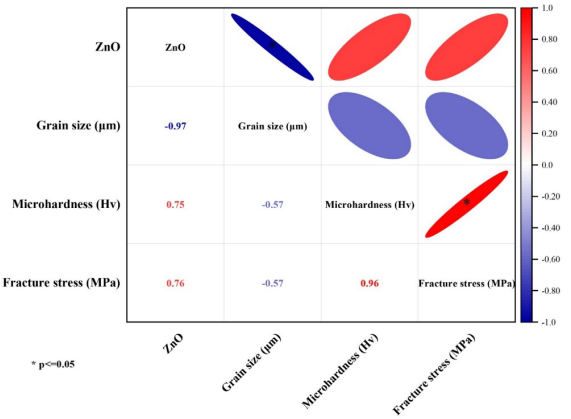

Figure 9. The correlation matrix representation of the results.

4. Conclusions

The significant effect of adding ZnO to the aluminosilicate BGs network (SiO_2-Al_2O_3-P_2O_5-CaF_2-CaO-K_2O-Na_2O) on the physicochemical properties of BGs was observed in the current study. Besides,

the incorporation of ZnO to BGs could successfully improve the mechanical properties of GIC samples. The mechanism behind the improvement of the mechanic properties of GICs related to decreasing the particles size and increasing the homogeneity of the ZnO-doped BGs samples; ZnO could diffuse to the Stern layer of BGs and increase its surface charge and homogeneity. The Tg of the aluminosilicate BGs was changed from 575 to 525 °C at the effect of doping BGs structure with ZnO. Besides, the grain size of the particle was reduced from 36 to 28 μm at the effect of the role of ZnO dopant on the particles' growth prevention. The microhardness of the GIC samples was increased from 677 Hv and 8.5 MPa to 816 Hv and 12.1 MPa, respectively, at the effect of increasing the amorphous phase and homogeneity of the ZnO-doped samples. In conclusion, this study suggested ZnO could improve the physicochemical properties of aluminosilicate BGs, and these samples are suggested as a good candidate for dental cement. Investigation of *in vitro* and *in vivo* properties of the fabricated samples was suggested for future studies.

Conflict of Interest

The authors declare no conflict of interest relevant to this article.

References

[1] S. Pagano, M. Chieruzzi, S. Balloni, G. Lombardo, L. Torre, M. Bodo, S. Cianetti, L. Marinucci, Biological, thermal and mechanical characterization of modified glass ionomer cements: The role of nano-hydroxyapatite, ciprofloxacin and zinc L-carnosine, Mater. Sci. Eng. C. 94 (2019) 76-85. https://doi.org/10.1016/j.msec.2018.09.018.

[2] T. De Caluwé, C.W.J. Vercruysse, I. Ladik, R. Convents, H. Declercq, L.C. Martens, R.M.H. Verbeeck, Addition of bioactive glass to glass ionomer cements: Effect on the physico-chemical properties and biocompatibility, Dent. Mater. 33 (2017) e186-e203. https://doi.org/10.1016/j.dental.2017.01.007.

[3] D.A. Kim, J.H. Lee, S.K. Jun, H.W. Kim, M. Eltohamy, H.H. Lee, Sol-gel-derived bioactive glass nanoparticle-incorporated glass ionomer cement with or without chitosan for enhanced mechanical and biomineralization properties, Dent. Mater. 33 (2017) 805-817. https://doi.org/10.1016/j.dental.2017.04.017.

[4] L.S. Bueno, R.M. Silva, A.P.R. Magalhães, M.F.L. Navarro, R.C. Pascotto, M.A.R. Buzalaf, J.W. Nicholson, S.K. Sidhu, A.F.S. Borges, Positive correlation between fluoride release and acid erosion of restorative glass-ionomer cements, Dent. Mater. 35 (2019) 135-143. https://doi.org/10.1016/j.dental.2018.11.007.

[5] J.W. Nicholson, S.K. Sidhu, B. Czarnecka, Enhancing the mechanical properties of glass-ionomer dental cements: A review, Materials (Basel). 13 (2020) 1-14. https://doi.org/10.3390/ma13112510.

[6] I.A. Moheet, N. Luddin, I.A. Rahman, T.P. Kannan, N.R. Nik Abd Ghani, S.M. Masudi, Modifications of Glass Ionomer Cement Powder by Addition of Recently Fabricated Nano-Fillers and Their Effect on the Properties: A Review, Eur. J. Dent. 13 (2019) 470-477. https://doi.org/10.1055/s-0039-1693524.

[7] J. Chen, Q. Zhao, J. Peng, X. Yang, D. Yu, W. Zhao, Antibacterial and mechanical properties of reduced graphene-silver nanoparticle nanocomposite modified glass ionomer cements, J. Dent. 96 (2020) 103332. https://doi.org/10.1016/j.jdent.2020.103332.

[8] I.A. Moheet, N. Luddin, I. Ab Rahman, S.M. Masudi, T.P. Kannan, N.R.N. Abd Ghani, Evaluation of mechanical properties and bond strength of nano-hydroxyapatite-silica added glass ionomer cement, Ceram. Int. 44 (2018) 9899-9906. https://doi.org/10.1016/j.ceramint.2018.03.010.

[9] L. Singer, Evaluation of the physico-mechanical properties of a new antimicrobial-modified glass ionomer cement Lamia Singer, (2021). https://bonndoc.ulb.uni-bonn.de/xmlui/handle/20.500.11811/9181.

[10] S. Mollazadeh, B. Eftekhari Yekta, J. Javadpour, A. Yusefi, T.S. Jafarzadeh, The role of TiO_2, ZrO_2, BaO and SiO_2 on the mechanical properties and crystallization behavior of fluorapatite-mullite glass-ceramics, J. Non. Cryst. Solids. 361 (2013) 70-77. https://doi.org/10.1016/j.jnoncrysol.2012.10.009.

[11] F.D. Haghighi, S.M. Beidokhti, Z.T. Najaran, S. Sahebian Saghi, Highly improved biological and mechanical features of bioglass-ceramic/ gelatin composite scaffolds using a novel silica coverage, Ceram. Int. 47 (2021) 14048-14061. https://doi.org/10.1016/j.ceramint.2021.01.274.

[12] X. Bao, F. Liu, J. He, Mechanical properties and water-aging resistance of glass ionomer cements reinforced with 3-aminopropyltriethoxysilane treated basalt fibers, J. Mech. Behav. Biomed. Mater. 116 (2021) 104369. https://doi.org/10.1016/j.jmbbm.2021.104369.

[13] T. Hasegawa, S. Takenaka, T. Ohsumi, T. Ida, H. Ohshima, Y. Terao, T. Naksagoon, T. Maeda, Y. Noiri, Effect of a novel glass ionomer cement containing fluoro-zinc-silicate fillers on biofilm formation and dentin ion incorporation, Clin. Oral Investig. 24 (2020) 963-970. https://doi.org/10.1007/s00784-019-

02991-0.

[14] Luddin N, Ching HS, Ab Rahman I, Kannan TP, Ghani NR. Cytotoxicity and Dentinogenic Potential of Nano-Hydroxyapatite-Silica Glass Ionomer Cement. Penerbit USM; 2021.

[15] I. Cockerill, Y. Su, S. Sinha, Y.X. Qin, Y. Zheng, M.L. Young, D. Zhu, Porous zinc scaffolds for bone tissue engineering applications: A novel additive manufacturing and casting approach, Mater. Sci. Eng. C. 110 (2020) 110738. https://doi.org/10.1016/j.msec.2020.110738.

[16] D. Skrajnowska, B. Bobrowska-Korczak, Role of zinc in immune system and anti-cancer defense mechanisms, Nutrients. 11 (2019). https://doi.org/10.3390/nu11102273.

[17] S. Mukherjee, Synthesis and Characterization of Trivalent al Substituted Zinc Ferrite using Ethylene Diamine (EDA) as Ligand, Non-Metallic Mater. Sci. 2 (2020) 8-14. https://doi.org/10.30564/omms.v2i2.1863.

[18] G.N. Elham, F. Kermani, M. Mashreghi, J.V. Khakhi, S. Mollazadeh, Interference of oxygen during the solution combustion synthesis process of ZnO particles: experimental and data modeling approaches, Ind. Eng. Chem. (2021). (currently under review).

[19] H. Aali, N. Azizi, N.J. Baygi, F. Kermani, M. Mashreghi, A. Youssefi, S. Mollazadeh, J.V. Khaki, H. Nasiri, High antibacterial and photocatalytic activity of solution combustion synthesized $Ni_{0.5}Zn_{0.5}Fe_2O_4$ nanoparticles: Effect of fuel to oxidizer ratio and complex fuels, Ceram. Int. 45 (2019) 19127-19140. https://doi.org/10.1016/j.ceramint.2019.06.159.

[20] L. Cormier, L. Delbes, B. Baptiste, V. Montouillout, Vitrification, crystallization behavior and structure of zinc aluminosilicate glasses, J. Non. Cryst. Solids. 555 (2021). https://doi.org/10.1016/j.jnoncrysol.2020.120609.

[21] F. Kermani, S.M. Beidokhti, F. Baino, Z. Gholamzadeh-Virany, M. Mozafari, S. Kargozar, Strontium-and cobalt-doped multicomponent mesoporous bioactive glasses (MBGS) for potential use in bone tissue engineering applications, Materials (Basel). 13 (2020) 1348. https://doi.org/10.3390/ma13061348.

[22] F. Kermani, A. Gharavian, S. Mollazadeh, S. Kargozar, A. Youssefi, J. Vahdati Khaki, Silicon-doped calcium phosphates; the critical effect of synthesis routes on the biological performance, Mater. Sci. Eng. C. 111 (2020) 110828. https://doi.org/10.1016/j.msec.2020.110828.

[23] F. Kermani, S. Mollazadeh, S. Kargozar, J.V. Khakhi, Solution combustion synthesis (SCS) of theranostic ions doped biphasic calcium phosphates ; kinetic of ions release in simulated body fluid (SBF) and reactive oxygen species (ROS) generation, Mater. Sci. Eng. C. 118 (2021) 111533. https://doi.org/10.1016/j.msec.2020.111533.

[24] D.S. Sanditov, M.I. Ojovan, On relaxation nature of glass transition in amorphous materials, Phys. B Condens. Matter. 523 (2017) 96-113. https://doi.org/10.1016/j.physb.2017.08.025.

[25] M.N. Azlan, M.K. Halimah, A.B. Suriani, Y. Azlina, S.A. Umar, R. El-Mallawany, Upconversion properties of erbium nanoparticles doped tellurite glasses for high efficient laser glass, Opt. Commun. 448 (2019) 82-88. https://doi.org/10.1016/j.optcom.2019.05.022.

[26] F. Kermani, S. Kargozar, Z. Tayarani-Najaran, A. Yousefi, S.M. Beidokhti, M.H. Moayed, Synthesis of nano HA/βTCP mesoporous particles using a simple modification in granulation method, Mater. Sci. Eng. C. 96 (2019). https://doi.org/10.1016/j.msec.2018.11.045.

[27] S. Mollazadeh, J. Javadpour, A. Khavandi, Biomimetic synthesis and mechanical properties of hydroxyapatite/poly (vinyl alcohol) nanocomposites, Adv. Appl. Ceram. 106 (2007) 165-170. https://doi.org/10.1179/174367607X168996.

[28] S. Kargozar, N. Lotfibakhshaiesh, J. Ai, M. Mozafari, P. Brouki, S. Hamzehlou, M. Barati, F. Baino, R.G. Hill, M. Taghi, Acta Biomaterialia Strontium-and cobalt-substituted bioactive glasses seeded with human umbilical cord perivascular cells to promote bone regeneration via enhanced osteogenic and angiogenic activities, Acta Biomater. (2017). https://doi.org/10.1016/j.actbio.2017.06.021.

[29] H. Kazemi, F. Kermani, S. Mollazadeh, J. Vahdati Khakhi, The significant role of the glycine-nitrate ratio on the physicochemical properties of CoxZn1−xO nanoparticles, Int. J. Appl. Ceram. Technol. 17 (2020) 1852-1868. https://doi.org/10.1111/ijac.13515.

[30] F. Kermani, S. Mollazadeh, S. Kargozar, J.V. Khakhi, Improved Osteogenesis and Angiogenesis of the Surface Functionalized Calcium Phosphates (CaPs): A State-of-the-Art Study, Mater. Sci. Eng. C. (2020).

[31] S. Shorvazi, F. Kermani, S. Mollazadeh, A. Kiani-Rashid, S. Kargozar, A. Youssefi, Coating Ti6Al4V substrate with the triple-layer glass-ceramic compositions using sol-gel method; the critical effect of the composition of the layers on the mechanical and in vitro biological performance, J. Sol-Gel Sci. Technol. 94 (2020). https://doi.org/10.1007/s10971-020-05233-y.

[32] E. Varini, S. Sánchez-Salcedo, G. Malavasi, G. Lusvardi, M. Vallet-Regí, A.J. Salinas, Cerium (III) and

(IV) containing mesoporous glasses/alginate beads for bone regeneration: Bioactivity, biocompatibility and reactive oxygen species activity, Mater. Sci. Eng. C. 105 (2019) 109971. https://doi.org/10.1016/j.msec.2019.109971.

[33] S. Kargozar, F. Kermani, S.M. Beidokhti, S. Hamzehlou, E. Verné, S. Ferraris, F. Baino, Functionalization and surface modifications of bioactive glasses (BGs): Tailoring of the biological response working on the outermost surface layer, Materials (Basel). 12 (2019) 3696-3714. https://doi.org/10.3390/ma12223696.

[34] F. Kermani, S. Mollazadeh, J. Vahdati Khaki, A simple thermodynamics model for estimation and comparison the concentration of oxygen vacancies generated in oxide powders synthesized via the solution combustion method, Ceram. Int. 45 (2019) 13496-13501. https://doi.org/10.1016/j.ceramint.2019.04.053.

[35] A. Flores, F. Ania, F.J. Baltá-Calleja, From the glassy state to ordered polymer structures: A microhardness study, Polymer (Guildf). 50 (2009) 729-746. https://doi.org/10.1016/j.polymer.2008.11.037.

[36] P. Barfi Sistani, S. Mollazadeh Beidokhti, A. Kiani-Rashid, Improving the microstructural and mechanical properties of in-situ zirconia-mullite composites by optimizing the simultaneous effect of mechanical activation and additives, Ceram. Int. 46 (2020) 1472-1486. https://doi.org/10.1016/j.ceramint.2019.09.113.

[37] J. Wegner, M. Frey, M. Piechotta, N. Neuber, B. Adam, S. Platt, L. Ruschel, N. Schnell, S.S. Riegler, H.R. Jiang, G. Witt, R. Busch, S. Kleszczynski, Influence of powder characteristics on the structural and the mechanical properties of additively manufactured Zr-based bulk metallic glass, Mater. Des. 209 (2021) 109976. https://doi.org/10.1016/j.matdes.2021.109976.

[38] N. Sohrabi, J. Jhabvala, R.E. Logé, Additive manufacturing of bulk metallic glasses—process, challenges and properties: A review, Metals (Basel). 11 (2021). https://doi.org/10.3390/met11081279.

[39] R. Haak, T. Näke, K.J. Park, D. Ziebolz, F. Krause, H. Schneider, Internal and marginal adaptation of high-viscosity bulk-fill composites in class II cavities placed with different adhesive strategies, Odontology. 107 (2018) 374-382. https://doi.org/10.1007/s10266-018-0402-1.

[40] Z. Mollaei, F. Kermani, F. Moosavi, S. Kargozar, J.V. Khakhi, S. Mollazadeh, In silico study and experimental evaluation of the solution combustion synthesized manganese oxide (MnO_2) nanoparticles, Ceram. Int. (2021). https://doi.org/10.1016/j.ceramint.2021.09.245.